DOI: 10.21608/ADJALEXU.2021.36047.1086

Characterization and Evaluation of Osseointegration of Modified PEEK Implants Using Nano-hydroxyapatite Particles: Laboratory and Experimental Study

Doaa M Aboul Azm[1]*BDs*, Sonia M Elshabrawy [2] *Ph.D*,Mostafa N Aboushelib [3]*Ph.D*, Hanaa M Ali [4]*Ph.D*, Emad A Soliman[5] *Ph.D*.

ABSTRACT

INTRODUCTION: Polyetherether ketone (PEEK) is a semicrystalline thermoplastic polymer that has been proposed as a substitute for metals in dental implants biomaterials because of its mechanical and biological properties.
OBJECTIVES: This study was aimed to prepare and characterize PEEK implant materials modified by different methods using nanoparticles of hydroxyapatite to overcome its limited bioactivity. The study also evaluated the ability of the modified PEEK implant to enhance osseointegration in a rabbit model.
METHODS: Four groups of PEEK specimens were prepared. Group1: specimens were constructed from untreated PEEK (control group), group2: specimens were coated with nanoparticles of hydroxyapatite (nHA) after etching the PEEK surfaces with sulfuric acid (98%) for one minute, group3: specimens were be coated with nanoparticles of hydroxyapatite (nHA) after PEEK surfaces treatment with Nd: YAG laser and group4: specimens were be constructed from melt-blended PEEK powder with nanoparticles of hydroxyapatite (nHA/PEEK). Each of the four groups were characterized by scanning electron microscope (SEM), Energy-dispersive X-ray (EXD), Fourier-transformed infrared spectroscopy (FTIR), X-ray Diffraction (XRD), contact angle measuring device and flexural strength test. The ability of each of the four groups to enhance bone osseointegration was evaluated in a rabbit model, by using histomorphometrical analysis.
RESULTS: Data was collected, summarized and statistically analyzed using the suitable methods.
CONCLUSION: PEEK biocompatibility and its chemical inertness can be improved with coating the surface with nano sized HA or mix blended of PEEK with nHA which does not affect its mechanical strength.
KEYWORDS: PEEK, hydroxyapatite, nanotopography, Laser.
RUNNING TITLE: Characterization evaluation osseointegration PEEK implants using nano-hydroxyapatite.

---

1 BDS, MS, Department of Dental Biomaterials, Faculty of Dentistry, Alexandria University, Egypt.
2 Professor of Dental Biomaterials, Department of Dental Biomaterials, Faculty of Dentistry, Alexandria University, Egypt.
3 Professor of Dental Biomaterials, Head of Dental Biomaterials Department, Faculty of Dentistry, Alexandria University, Egypt.
4 Professor of Oral Biology, Department of Oral Biology, Faculty of Dentistry, Alexandria University, Egypt.
5 Professor of Polymer Science and Technology, Head of Department of Polymeric Materials Research, City of Scientific Research and Technology Applications, New Borg El-Arab City, Alex. Egypt.

**Corresponding author:*
Email: doaadent@gmail.com

INTRODUCTION

Endosseous dental implants have dramatically changed the ways to replace the missing teeth with a high success rate which is determined by the ability of the implant materials to be well integrated with the surrounding bone (1).
The dental implants firstly were constructed from pure titanium (Ti), but it was too soft so, Ti alloys were developed to overcome their negative properties(2). However various complications can be associated with Ti implants such as hypersensitivity and high elastic moduli of a titanium implant compared to the surrounding bone which may cause stresses at the implant-bone interface due to load transfer resulting in peri-implant bone loss (2). Moreover, Ti has an esthetic problem because of lack of light transmission which results in a dark color of peri-implant soft tissue in case of thin biotype mucosa or mucosal recession around the Ti implant (3).
Ceramic implants were suggested as an alternative to overcome Ti drawbacks as well as increasing the demand of completely metal-free dental reconstructions. Yttrium stabilized tetragonal polycrystalline zirconia(Y-TZP) implants were shown to stimulate osseointegration, have low plaque affinity and can have a natural tooth color appearance (4) but again, the difference in elastic moduli between implants and their surrounding bone could lead to peri-implant bone loss (5). The elastic modulus of Ti is found to be 110 GPa and for zirconia is 210 GPa which are 5-14 times higher than that of human bone (6-18 GPa) (5).

Since the 1980s (6) the interest in polyetherether ketone (PEEK) has seen increasing as a substitute to metal and ceramic implants, due to its mechanical and biological properties (7) in addition to its translucency to X-rays.

Polyetherether ketone has stable physical and chemical properties (8) as it has wear-resistant and stable at high temperatures (9) as well as it remains stable in sterilization processes (10). Also it has a high biocompatibility in vitro and in vivo so, it doesn't cause any clinical significant inflammations (11). Moreover, it has elastic modulus which is close to that of human bone so it reduces the stress concentrations around the implant so, can be used in spinal and orthopedic surgery (12). Recently, there has been an interest in improving PEEK biocompatibility, which can be done by incorporating bioactive materials such as hydroxyapatite (HA) into the polymer (13), surface modifications, or by making porous PEEK-HA as a scaffold for bone ingrowth (14).

Modifications of the implant surface can enhance growth of the osteoblasts so, the bone integration could be improved. Nanohydroxyapatite (nHA) particles as a bioactive coating material have been used frequently with Ti dental implants, and it is interesting as its chemical structure is similar to the minerals in the bone (15) allowing for a faster osseointegration as it has strong osseoconductive properties when used as a coating around implants (16, 17). Thus in this study PEEK implants will be coated or mix blended with bioactive nanohydroxyapatite particles (nHA) to improve the surface roughness in order to stimulate the osseoconductive properties (18).

Rationale

As dependency on dental implants as treatment options is increased, new materials with improved biological, mechanical properties, more economic and extending lifetime by eliminating corrosion, are needed.

The null hypothesis would be that both PEEK surface coated or mix blended with bioactive nHA particles could enhance the PEEK biocompatibility to achieve early osseointegration, but coatings may exhibit high adhesion strength of osteoblasts to PEEK implants.

MATERIALS AND METHODS

This study was divided into two sections: Laboratory study (preparation and characterization of biomaterials) and experimental study (assessment of biomaterials osseointegration). Nanohydroxyapatite was synthesized using wet chemical precipitation reaction according to the method of Pier Giorgio and his coworkers (19). Two types of nHA/PEEK-based biomaterials were prepared. The first type was based on coating surface-treated PEEK specimens with pre-prepared nHA. Meanwhile, the second type was based on nHA/PEEK composites. Such specimens will be categorized into four groups which will be encoded and listed in table (1).

Table.1: Code and number of each group of PEEK and nHA/PEEK-based specimens

Group	Specimens	Code of Specimens	No.of Specimens for lab work	No.of Specimens for experimental work
1	PEEK specimens	PEEK	25	8
2	nHA-coated acid-etched PEEK-based specimens	nHA/AE-PEEK COAT	25	8
3	nHA-coated laser-irradiated PEEK-based specimens	nHA/LI-PEEK COAT	25	8
4	nHA-PEEK composite-based specimens	nHA-PEEK COMP	25	8

The specimens for first three groups were made from medical grade PEEK disc (JUVORATM Ltd, Lanchire, UK) using CAD/CAM system (DGSHAPE. DWX.520, Japan) then, they were finished and polished with series of silicon carbide abrasive papers with increasing coarseness. Afterward, the polished specimens were rinsed with deionized water in ultrasonic bath for 60 seconds and then dried overnight prior to surface treatment.

All the specimens were sandblasted using aluminum oxide (AL2O3) particles with diameter of 45 µm, pressure 2.8 bar and at the distance of 1 cm for time 15 seconds.

Sandblasted PEEK specimens of second group were etched with concentrated sulfuric acid (98%) by immersing them for 1 minute then, rinsing with deionized water for 1 minute (20).

Sandblasted PEEK specimens of third group were immersed in distilled water for 2 min followed by immersing in pure propyl alcohol for 3 min then, they were ultrasonically cleaned by immersing them in distilled water for around 5 min. The specimens were then thoroughly dried using tissue followed by air prior to laser treatment. The surfaces of cleaned dried specimens were directly irradiated in laser irradiator (PL8000, Contiuum laser company, USA) with Nd: YAG laser beam with the wavelength of 1064 nm for 1 min. at 10 mj/pulse power setting and 10 Hz frequency in a non-contact mode at a working distance of 20 cm.

The acid-etched and laser-irradiated specimens were coated with nHA according to the procedure described in patent SE 527610 (21). PEEK specimens were washed with isopropanol before coating procedures to remove debris.

Formation of nHA coatings onto specimens was achieved in two steps; the first step was concerning the preparation of the nHA coating-forming suspensions by dispersing hydroxyapatite nanoparticles in 20 ml of absolute ethanol followed by placing in an ultrasonic bath at room temperature for 5 min to assure good dispersion and nanoparticles disintegration. In the second step, the targeted surface-treated specimens were immersed into the pre-prepared coating-forming suspension. The immersed specimens were rotated at 6000 rpm for one minute using homogenizer (Ultra Turrax T-18, Japan). Afterward, PEEK specimens soaked in nHA suspension were removed and

then dried in the oven at 325 °C for 5 minutes. Finally, they left to be cool at room temperature.

Construction of nHA/PEEK composite for group four was first achieved by mixing (physically blended) hydroxyapatite nanoparticles with PEEK powder (Merck. Darmstadt, Germany) at volume ratio of 1:10 using a planetary ball mill (Retsch ball mill EMAX) under room temperature.

Thermoforming of milled nHA/PEEK was done using compression molding technique. The milled nHA/PEEK powder was filled in cavity of specially designed thermo-stable mold made from corrosion resistant stainless steel (Such mold is constructed from three plates; base, a middle plate containing the bar-shaped mold cavities (20mm × 4 mm ×1.5 mm) for laboratory study and implant mold cylinder cavities (8mm x 3.3mm) for experimental study, and fitting covering plate.

The mold filled with milled nHA/PEEK powder was placed between the two plates of home-made hydraulic hot pressing machine (Koosha hydraulic press) and applied to high pressure (350 bar) to cold press the composite-forming powder. The hot press machine plates were heated to 410°C at a rate of 10°C/min and pressure of ~20bar. Once reaching the set temperature, the plates was held at constant temperature and pressure for 10 min to assure homogeneity of the melt. Afterward, high pressure of 150bar was applied with switching off the heating and was allowed to cool down naturally to room temperature. Finally, the mold plates were opened and specimens were released.

Characterization

The structural, morphological, and surface properties of nHA, pristine PEEK, nHA-coated surface-treated PEEK, and nHA/PEEK composite were characterized via the following laboratory analytical methods and measurements:

ATR-FTIR spectral analysis

Chemical analysis and identification of nHA, PEEK, nHA/PEEK based- specimens were taken place using FTIR spectroscopy. All specimens were first placed in a desiccators containing silica gel for at least 48 hours at room temperature to make sure the presence of minimal moisture content before spectroscopic analysis. These specimens were examined using a spectrometer (Shimadzu 8400S, Japan) with a Golden Gate diamond horizontal attenuated total reflectance (ATR) system (ATR-8400M, Shimadzu Co, Ltd, Tokyo, Japan) was used. The spectra (32 scans at 2 cm-1 resolution) were recorded with the frequency range of 500-4000 cm-1. The incidence angle for the ATR crystal was 45°.

Transmission electron microscopy (TEM)

The morphological features of nHA were examined by TEM (JOEL- JEM 2100 plus, Tokyo, Japan).

X-ray diffractometric (XRD) analysis

To evaluate the atomic spacing and crystallinity of nHA and pristine PEEK and nHA/PEEK based- specimens, respectively. X-ray diffractometric analysis was performed using XRD diffractometer (Shimadzu XRD-7000 diffractometer Shimadzu Co. Ltd, Japan) (30 kV, 30 mA) with Cu K, Ni radiation and using computer software (DP-D1, Shimadzu Co. Ltd).

The specimen was scanned from 4 - 60° at a rate of 2°/min. The crystallinity was calculated by separating intensities due to presence of the amorphous and crystalline phases on the diffraction phase as the computer-aided curve resolving technique was used to separate crystalline and amorphous phases of diffractogram.

Scanning electron microscope (SEM)

The morphological features and microstructures of nHA, PEEK and nHA/PEEK-based specimens were examined by a scanning electron microscope (JEOL 6360LA Ltd., Rigaku, Tokyo, Japan). The specimens were fixed on stainless steel stubs using double-sided tape. A very thin layer of gold was sputtered on them to enhance their electrical conductivity by sputter (JOEL JFC-1100E Ltd., Tokyo, Japan). The gold coated-specimens were subjected to microscopic examination at an acceleration voltage of 25 kV with a magnification of 500-1000×.

Energy dispersive X-ray (EDX)

Elemental analysis of pristine PEEK and nHA/PEEK-based biomaterials were carried out using energy dispersive X-ray analysis.

Contact angle measurement

A goniometer (Ramé - hart, model 500-F1, France) was used to measure the contact angle between the surface of PEEK and nHA/PEEK-based biomaterials and the tangent to the surface of the liquid droplets (deionized water) by using the static sessile drop method that, express the surface hydrophilicity or wettability of the object. Surface wettability was measured using deionized water based on a droplet (4 μL) suspended from an automatic piston syringe that was allowed to fall freely onto the object surface at room temperature and photographed using high snapshot camera after 5 seconds. An image analyzer was used to measure the contact angle formed between the surface of the object and the droplet of water using a circular algorithm technique. Five measurements were taken for each specimen and the average was calculated.

Flexural strength testing

Flexural strength of PEEK and nHA/PEEK-based biomaterial specimens was measured using a universal testing machine (Shimadzu AG-IS, Shimadzu Co. Ltd., Japan) according to the Plastics Determination of flexural strength testing standard, International Organization for Standardization (ISO 178) (22).

Twenty-eight (n=28) microbar-shaped specimens, seven for each group (n=7) with 20 mm length, 4 mm width, and 1.5 mm thickness were used for each of the four biomaterials groups. Three-point bending test was used to calculate the flexural strength of the specimens through stress- strain curve. The specimens were subjected to flexural strength test in a universal testing machine at a speed of 5 mm/min until maximum bending. The maximum load (F, in Newton) of each specimen was obtained and flexural strength (**σ**) was calculated according to Plastics Determination of flexural properties (ISO 178: 2010.https:// www.iso.org/ standard/ 45091. Html) as follows:

$$\sigma = 3FL/2bd^2$$

Where:
F: The load (force) at the fracture point (N)
L: The length of the support span
b: The width
d: The thickness

Experimental (in vivo) work

This animal study was conducted after receiving the approval of the Ethical Committee [IRB NO 00010 556-IORG 0008839] at Faculty of Dentistry, Alexandria University, Egypt.

Sixteen Spain male line V white rabbits were used, with an age of six months (weighed from 2.5 to 3 kilograms) and were in a good systemic health. They were fed in the animal house on a soft diet and multi-vitamins; A, D3 & E were added to their drinking water at dose of 1 ml/ L for two weeks before surgery.

The rabbits were divided into four groups (4 in each group) according to the implant inserted. Two specimens of each type of the pre-prepared implants (3.3 mm x 8 mm) (23) were inserted in each rabbit; one in the right femur and the other in the left one. Four types of implant specimens were used in this work:

- Group 1: Untreated PEEK implant specimens (n=8).
- Group 2: PEEK specimens coated with nHA after surface etching with sulfuric acid (n=8).
- Group 3: PEEK specimens coated with nHA after laser irradiation to the surface (n=8).
- Group 4: Specimens prepared from PEEK blended with nHA (n=8).

Surgical and implantation procedures

Surgical procedures were taken place under general anesthesia and in aseptic conditions. Rabbits were anesthetized with intramuscular injection of Ketamine in combination with xylazine at a dose of 35 mg/kg and 5 mg/kg of body weight respectively. Surgical site (the hind legs at the head of the femur) was shaved using a blade to expose the skin that was decontaminated with Betadine (El-Nile Company for Pharmaceutical and Chemical industries Cairo, Egypt). The skin incision of about 3 cm was made using no. 15 blade in the lateral side of the skin at the surgical site. The periosteum was reflected with a periosteal elevator and the bone was exposed (Figure 1A).

The implant site was prepared using low-speed rotary and profuse saline irrigation while drilling with a minimum amount of trauma. Intermittent and sequential drilling of implant created socket was continued until reaching the same diameter and length of the implant (3.3 mm x 8 mm) (Figure 1B). The implant was inserted into the created socket in dorsoventral direction with finger pressure, followed by its full insertion with gentle pressure and screwed into the bone (Figure 1C&D). After implant insertion all reflected muscles were subsequently repositioned and the fascia was sutured with catgut absorbable surgical sutures, followed by skin repositioned and incision closure with silk nonabsorbable surgical sutures (Figure 1 E&F). The silk sutures were removed after one week.

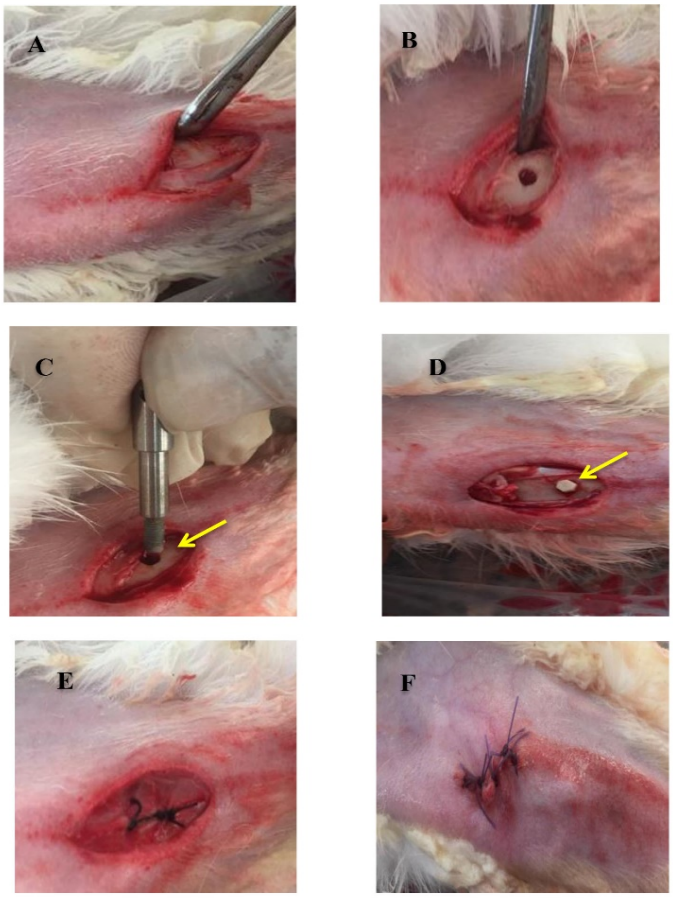

Figure 1: Surgical and implantation procedures:
(A) Reflection of femoral muscles and exposure of femur head.
(B)Implant socket after complete drilling.
(C&D) Implant insertion into surgicaly created socket (arrows).
(E) Fascia sutured with absorbable surgical sutures.
(F) Skin repositioned with silk nonabsorbable surgical sutures

To avoid any infection and pain, postoperative intramuscular injection of broad-spectrum antibiotic (Cefotax 250 mg.Pharmaceutical Industrial CO. EPICO. Egypt) and analgesic (Voltaren 75 mg. NOVARTIS Pharma S.A.E. Egypt) were administrated every 72 hours for 10 days. Then the rabbits were monitored daily for weight gain and cage behavior.

The implants sites were allowed to heal for 6 weeks according to the finger of osseointegration for animal models (24, 25), and then the animals were euthanized with an overdose of sodium pentobarbital (60 mg/mL.1 ml/kg intravenously) (26). The distal heads of the femurs containing the implants of all groups were dissected out with a surgical saw. All soft tissues attached to them were removed for preparation of the non-decalcified histological sections to investigate peri-implant bone healing and osseointegration.

Preparation of non-decalcified bone sections (27)

Fixation of the specimens was done by immersing them in 10% neutral-buffered formalin solution for 7 days and then the specimens were dehydrated with ethanol in increasing concentrations (70%, 80%, 90%, and 100%). The dehydrated bone specimens were immersed into xylene for 24 hours at room temperature. Each specimen was

embedded in transparent methyl methacrylate resin (Figure 2). After complete polymerization, non-decalcified sections were cut down to blocks. Such blocks were sectioned in a transverse direction, perpendicular to the axis of the implants (28). The thickness of the specimens was adjusted to approximately 70–80 µm using microtome (Metkon, Micracut 150, precision cutter BURSA, Turkey). The resulted sections were smoothened using sandblasting papers to remove all scratches followed by their polishing using a suspension of alumina polishing particles. Then the polished sections were washed with distilled water and allowed for air drying. Non-decalcified sections were stained with Stevenl's blue, and then counter stained with Van Gieson picro -fuchsin (29).

Figure 2: FTIR results of hydroxyapatite nanoparticles

Statistical analysis

The Kolmogorov-Smirnov test was used in order to verify the normality of distribution. Quantitative data were described using range (minimum and maximum), mean, standard deviation, median and IQR. F-test (ANOVA) was used to compare between the four studied groups.

RESULTS

1-Characterization results of nHA

Fourier Infrared Spectroscope (FTIR) results for nHA

The FTIR spectra of HA nanoparticles (Figure 3) showed the absorption peaks for various groups between 4000–400 cm-1. The peaks that were present at 3400–3700 cm-1 corresponds to the OH- absorption, whereas 2600–2400 cm-1 show hydrogen-bonded salts (30). The peaks at 1653 cm-1 and 1470 cm-1 represented CO3-2.The bending mode of O-P-O of HPO4-3 were found at 561 cm1 (31). The presence of the PO4-3 group was assigned at peak of 597 cm-1 (32). The medium stretching vibration was observed at 1325 cm-1 due to the presence of the C=O group.

Transmission Electron Microscopy (TEM) results of nHA

TEM observations (Figure 4) revealed that all the precipitated powders are of nano-sized needle-like particles of HA. Certain agglomeration of nHA particles was observed.

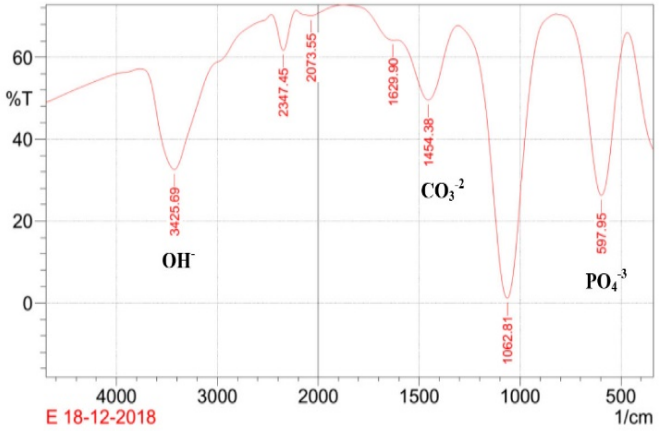

Figure 3: TEM images of hydroxyapatite nanoparticles.

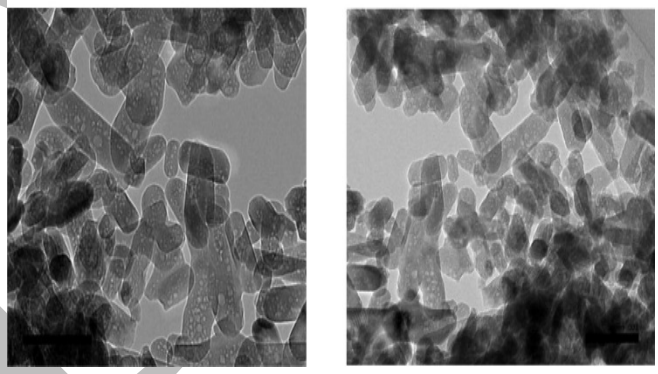

Figure 4: SEM images of PEEK surfaces.
(A) gp1 no surface treatment.
(B) gp 2 surface treatment with sulfuric acid then coating with nHA.
(C) gp 3 surface treatment with laser then coating with nHA.
(D) gp4 bioactive PEEK nano-composites. Scale bars: 10 µm. Magnifications: 1000x- 5 µm. Magnifications: 5000x

X-ray Diffraction (XRD) analysis for nHA

XRD analysis of hydroxyapatite nanoparticles was matched with HA reference code (00-009-0432). The resulted XRD pattern revealed the specific peaks for HA crystals phase which were represented by (211), (112), and (300).

2. Characterization results of PEEK specimens

Scanning Electron Microscope (SEM) results for PEEK specimens

Scanning electron micrographs with magnifications 1000x and 5000x (Figure 5) revealed significant change on the surface morphology of PEEK samples of the second and the third groups (Figure 5B) and (Figure 5C). Comparing with the untreated control group (Figure 5A), the presence of the crystals of nHA coating with a random arrangement was observed. In group four (Figure 5D) the particles of nanohydroxyapatite can be observed within PEEK bioactive nanocomposites particles.

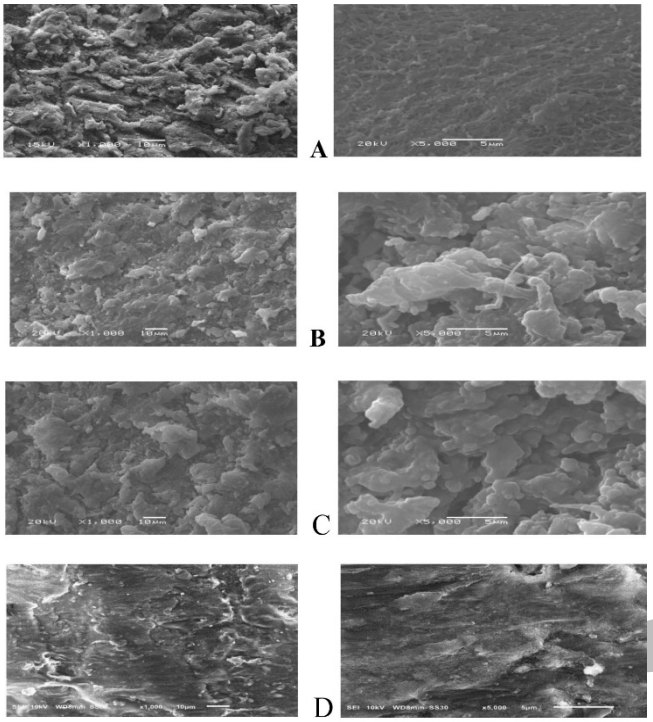

Figure 5: Energy-dispersive X-ray (EDX) analysis

X-ray Diffraction (XRD) results

The XRD results of the PEEK were exhibited both sharp and broad features because it is a semicrystalline material (a mixture of amorphous and crystalline). The sharp peaks were related to the crystalline component and the broad features were related to the amorphous component. As the crystallite size is reduced, the diffraction peaks broaden. The patterns of PEEK polymer with surface treatment showed the specific peaks with decreased intensity for the diffraction peaks of PEEK specimen after sulfuric acid (group 2) or laser treatment (group 3). The specific peaks of PEEK were still present in PEEK specimens without treatment and after surface treatment. XRD patterns of pristine PEEK exhibits characteristic peaks at around 2θ = 18.8◦, 20.7◦, 22.9◦ while the patterns of PEEK/ nanocomposites showed an additional peak at 29.2 ◦ due to the reflection of nanocrystals.

Fourier Infrared Spectroscopy (FTIR) results for PEEK specimens

The samples of PEEK were analyzed using the FTIR (Shimadzu FTIR-8400 S, Japan). Comparing to earlier FTIR studies undertaken by Chalmers et al (33), the similarities of the spectra were clearly evident as the finger-print region of the spectrum (1700cm-1 – 650cm-1) exhibited the distinctive spectral features typical to an FTIR recorded spectra of PEEK.

The stretching vibration peak for C=O was at 1649.80 cm-1; the aromatic ring framework vibration peak was at 1597.62 cm-1 and 1490.41 cm-1; bending vibration absorption peaks for C-H out of the benzene ring plane was at 767.34 cm-1, meanwhile, at 836.92 cm-1 was the specific peak of aromatic ring paraposition substitution; from this analysis, it could be confirmed that there was PEEK in the sample.

Absorption peaks at 939.36 cm-1 and 1037.74cm-1 are corresponding to the key band of PO4-3, absorption peaks at 560.34 cm-1, and 603.75cm-1 belong to the bending vibration peaks of PO4-3. From this analysis, it could be confirmed that there was HA in the sample.

Energy-dispersive X-ray (EDX) results

Energy-dispersive X-ray analysis (Figure 6) provides elemental analysis on areas of nanometers in diameter. EDX results for group 1 (untreated PEEK specimens) revealed that, the chemical structure of specimens included carbon (C) and oxygen (O) but, for groups 2, (coated PEEK with nHA after etching by sulfuric acid), group3 (coated PEEK with nHA after laser treatment) and group 4 (nHA/ PEEK composite), the chemical structure of specimens included carbon C, oxygen O, calcium Ca, and phosphorus P.

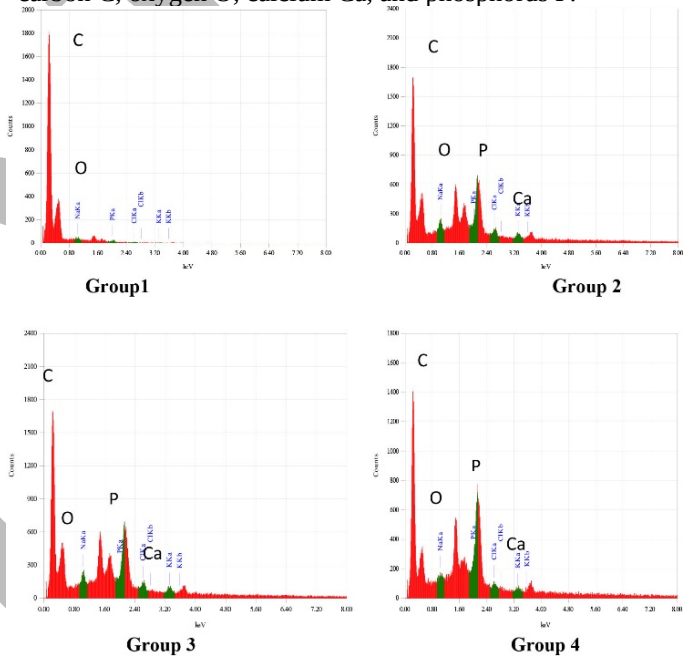

Figure 6: Photomicrographs of the lamellar bone tissue around the PEEK implants after 6 weeks of healing.
(A) Control uncoated group 1,
(B) nHA-coated implant after acid etching group 2,
(C) nHA- coated implant after laser treatment group 3 and
(D) nHA/PEEK composite implant group 4.
Note the amount of fibrous tissue in the gaps between the new bone and implant surfaces (arrows). Non-decalcified stained sections with Stevenl's blue stain counterstained with van Gieson picro-fuchion. Original magnifications 100x.

Contact angle test results

In this work, the mean value of contact angle of untreated PEEK (group 1) was about 76.59 ±17.18. Moreover, etching with sulfuric acid (group 2) generated a significantly rougher, more porous surface than the laser surface treatment (group 3) and this is expected to compromise its wettability which is became more than untreated PEEK specimens (mean value of contact angle of group two was about 73.17 ±9.15. While, mean value of contact angle of group3 was 73.77 ± 8.09). The wettability of PEEK /HA nanocomposite specimens (group4) was markedly increased

compared with the other three groups (mean value of contact angle for group 4 was 63.66 ±3.63).

Flexural Strength test results

All PEEK microbars of the untreated PEEK (group1) (mean value of max. fracture force was 86.25 ±17.23) or surface etching whether by sulfuric acid (group 2) (mean value of max. fracture force was 73.79 ±15.91) or laser (group 3) (mean value of max. fracture force was 78.25 ±14.78) showed gradual bending till the maximum deflection capacity of the material without fracture. The microbars specimens of PEEK /HA nanocomposite (group 4) were fractured when reaching maximum deflection capacity (mean value of max. fracture force was 77.81 ±10.48).

3. Histological results

Histological evaluation of nondecalcified sections

The qualitative histological evaluation of non-decalcified sections after 6 weeks of healing revealed stained mature lamellated bone close to the implant surface (Figure 7). All implants were osseointegrated. However, the nHA/ PEEK-based implants were almost integrated well with the surrounding bone tissue with only sparse amounts of fibrous tissue have been observed between the implant surface and new bone formed (Figure 7B-D) but, in non-coated PEEK implants (group 1), more amount of fibrous tissue (Figure 7A) was observed between the implant and bone. Signs of osteoconduction of nHA/ PEEK implants were observed as most of the threads and implant surfaces were covered with mature bone formed of Haversian systems and enclosing arranged osteocytes. No immunological cells as a sign of an inflammatory response were observed near to the implanted materials.

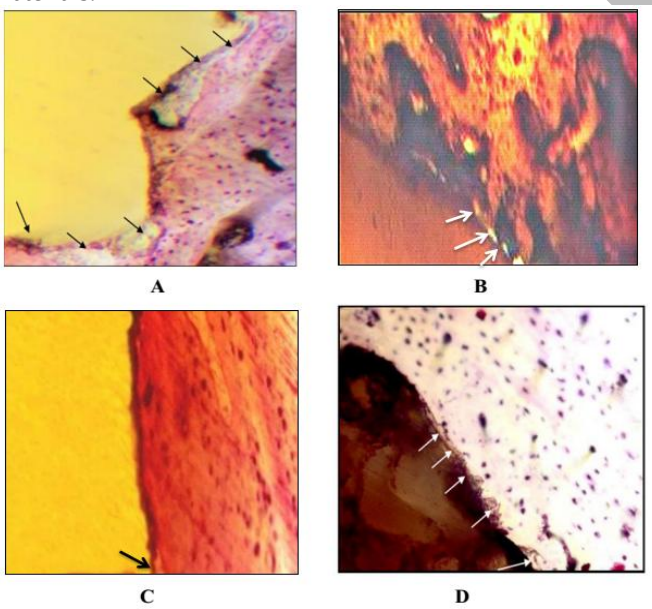

Figure 7: Photomicrographs of the lamellar bone tissue around the PEEK implants after 6 weeks of healing.
(A) Control uncoated group 1,
(B) nHA-coated implant after acid etching group 2,
(C) nHA- coated implant after laser treatment group 3 and
(D) nHA/PEEK composite implant group 4. Note the amount of fibrous tissue in the gaps between the new bone and implant surfaces (arrows). Non-decalcified stained sections with Stevenl's blue stain counterstained with van Gieson picro-fuchion. Original magnifications 100x.

Histomorphometric results

The quantitative evaluation of bone-implant contact (BIC) of the histological non decalcified sections revealed newly formed bone in close contact with the implant surface. The means and standard deviations (±SD) of bone-implant contact percentage (BIC %) for the four studied groups were indicated no significant difference (F=0.431, P> 0.05). The mean ± (SD) of the BIC% was 66.13 ± 14.77% for the control (uncoated) group, 73.0 ± 18.62% for nHA/bioactive–coated surfaces after acid etching (group 2), 75.13 ± 19.22% for nHA/bioactive–coated surfaces after laser treatment (group 3), and 69.50 ± 15.15% for nHA/ PEEK composite implants (group 4).

The BIC% was higher in coated implants than nHA/ PEEK composite implants compared to a control group. The BIC% of coated implants surface after laser treatment is slightly higher than that of coated implant surfaces after acid etching.

DISCUSSION

As PEEK has excellent properties such as mechanical strength and chemical resistance, it can be applicable for dental implants and has already been employed to replace metallic implant components as it has an elastic modulus close to that of the bone(2). But, it is an inert material which suffers from poor osseointegration due to presence of polyester functional groups and an aromatic ring in its chemical structure that make it hydrophobic and resistant to protein and cell adhesion.

Osseointegration could be stimulated by surface modification of PEEK by using bioactive materials that enhance its adhesion to bone tissue. Recent studies have suggested surface modifications as new processing that could improve the biological properties of pure PEEK which might increase the surface energy and enhance matrix protein adsorption, bone cell migration, proliferation, and finally enhance osseointegration (34).

Hydroxyapatite nano-particles (nHA) was used as a bioactive material which provides a more suitable environment for cell growth and protein attachment as nHA is more hydrophilic than PEEK due to presence of hydroxyl group in its structure.

The effect of nHA on PEEK implants was evaluated in this study and it has been found that there was an increase in bone-implant contact than uncoated ones.

Nano-scale hydroxyapatite was synthetized using wet chemical precipitation method from aqueous solutions, which is one of the most common techniques used for preparing nHA due to its simplicity.

Surface treatment of PEEK by etching with 98% sulfuric acid or laser irradiation before coating with nHA was used to modify its surface as roughness and wettability of the surface were increased and increase cell adhesion in PEEK-based implant (35).

The surface roughness of coated specimens after laser irradiation in this study seemed to be more effective than coated specimens after acid etching due to formation of craters at the points of laser occurrence but the craters created after acid etching had larger width and depth, however nHA/ PEEK bioactive composite specimens

showed decreased surface roughness due to the presence of nano-size hydroxyapatite crystals. The enhancement in osseointegration is due to improving the biological responses at the bone-implant interface not due to the absorption of HA nano-particles.

The increased BIC% after 6 weeks of healing after insertion was higher in nHA/ PEEK implants than the control uncoated implants (group 1) but without significant difference.

In this study, the histological and histomorphometric analysis showed that surface coating with nHA particles seemed to improve PEEK bioactivity more than nHA/ PEEK composite as nHA was embedded rather than free and there was no covalent bond formation between nHA and the PEEK matrix so the release of calcium ions into the surrounded environment was not significantly increased (36).

In this study, it was found that modification of PEEK implant by surface coating or incorporation with bioactive materials (nanohydroxyapatite) improved the biocompatibility of PEEK and enhanced cell adhesion and proliferation so achieved early osseointegration more than uncoated PEEK implants.

These findings coincided with the proposed hypothesis for this research work and also have been confirmed by previous studies evaluating the modification of PEEK implant by nHA as bioactive material to enhance its osseointegration (36).

Rabbits were used in this study as they can be easily handled and they develop and reach skeletal maturity fast which is completed at the age of twenty-eight weeks (37- 39).

CONCLUSIONS

This study demonstrated that coating the surface of the PEEK implants or mix blended of PEEK powder with nHA could improve the BIC and demonstrated strong osseoconductive properties of PEEK implants in rabbit femur.

Surface treatment of PEEK implant with laser before coating is more effective than etching with sulfuric acid as BIC% revealed increased osseointegration.

Coating the surface of PEEK implant with nHA could enhance osseointegration more than nHA/PEEK biocomposite.

CONFLICT OF INTERESTS

There is no conflict of interests to declare in this work

REFERENCES

1. Zupnik J, Kim S-W, Ravens D, Karimbux N, Guze K. Factors associated with dental implant survival: a 4-year retrospective analysis. J Periodontol. 2011;82:1390−5.
2. Schwitalla A, Müller WD. PEEK Dental Implant: A Review of the Literature. J Oral Implantol. 2013; 39:743-9.
3. Andreiotelli M, Wenz HJ, Kohal R. Are ceramic implants a viable alternative to titanium implants?. A systematic literature review. Clin Oral Implants Res. 2009;20:32-47.
4. Kohal R, Klaus G, Strub J. Zirconia-implant-supported all-ceramic crowns withstand long-term load: a pilot investigation. Clin Oral Implants Res. 2006;17:565-71.
5. Huiskes R, Weinans H, Van Rietbergen B. The Relationship between stress shielding and bone resorption around total hip stems and the effects of flexible materials. Clin Ortho Relat Res. 1992;274:124-34.
6. Williams DF, McNamara A, Turner RM. Potential of polyetherether ketone (PEEK) and carbon-fibre - reinforced PEEK in medical app lications. J Mater Sci Lett. 1987;6:188-90.
7. Kurtz SM, Devine JN. PEEK biomaterials in trauma, orthopedic, and spinal implants. Biomaterials. 2007;28:4845-69.
8. Wang H, Xu M, Zhang W, Kwok DT, Jiang J, Wu Z, et al. Mechanical and biological characteristics of diamond-like carbon coated poly aryl-ether-ether-ketone. Biomaterials. 2010;31:8181–7.
9. Eschbach L. Nonresorbable polymers in bone surgery. Injury. 2000;31:22–7.
10. Williams D. Polyetheretherketone for long-term implantable devices. Med Device Technol. 2008;19:10–1.
11. Harsha AP, Tewari US. The effect of fiber reinforcement and solid lubricants on abrasive wear behavior of polyetherether ketone composites. J Reinf Plast Compos. 2003;22:751-67.
12. Skinner HB. Composite technology for total hip arthroplasty. Clin Ortho Relat Res. 1988;235:224-36.
13. Abu Bakar MS, Cheng MH, Tang SM, Yu SC, Liao K, Tan CT, et al. Tensile properties,tension-tension fatigue and biological response of polyether ether ketone-hydroxyapatite composites for load-bearing orthopedic implants. Biomaterials. 2003;24:2245-50.
14. Tan KH, Chua CK, Leong KF, Cheah CM, Cheang P, Abu Bakar MS, et al. Scaffold development using selective laser sintering of polyether etherketone – hydroxyapatite biocomposite blends. Biomaterials. 2003;24:3115-23.
15. Gottlander M, Albrektsson T, Carlsson LV. A histomorphometric study of unthreaded hydroxyapatite-coated and titanium-coated implants in rabbit bone. Int J Oral Maxillofac Implants. 1992;7:485-90.
16. Soballe K, Overgaard S. The current status of hydroxyapatite coating of prostheses. J Bone Joint Surg Br. 1996;78:689-91.
17. Zhu X, Eibl O, Scheideler L, Geis-Gerstorfer J. Characterization of nanohydroxyapatite/ collagen surfaces and cellular behaviors. J Biomed Mater Res A. 2006;79:114-27.
18. Ha SW, Gisep A, Mayer J, Wintermantel E, Gruner H, Wieland M. Topographical characterization and micro structural interface analysis of vacuum-plasma- sprayed titanium and hydroxyapatite coatings on carbon fibre-reinforced polyether ether ketone. J Mater Sci Mater Med. 1997;8:891-6.

19. Piergiorgio G, Caroline J, Cheryl A. Miller, Robert M, Paul V. Hatton. Process optimisation to control the physico-chemical characteristics of biomimetic nanoscale hydroxyapatites prepared using wet chemical precipitation. Materials. 2015;8:2297-310.
20. Patrick R, Bogna S, Marco W, Thomas A, Christoph HF, Jens F. Effect of different surface pretreatments and luting materials on shear bond strength to PEEK. Dent Mater. 2010;26:553–9.
21. Barkarmo S, Wennerberg A, Hoffman M, Kjellin P, Breding K, Handa P, et al. Nano-hydroxyapatite-coated PEEK implants: A pilot study in rabbit bone. J Biomed Mater Res A. 2013;101:465-71.
22. Plastics Determination of flexural properties. ISO178: 2010. Available at: https:// www.iso.org/ standard/ 45091. Html.
23. Liu Y, Zhou Y, Jiang T, Zhang Z, Wang YN. Evaluation of the osseointegration of dental implants coated with calcium carbonate: an animal study. Int J Oral Sci. 2017;9:133–8.
24. Takayuki M, Salvi GE, Offenbacher S, Felton DA, Cooper TF. Cells and matrix reactions at titanium implants insurgically prepared rat tibiae. Int J Oral Maxillofac Implants. 1997;12:472-85.
25. Buser D, Schenk RK, Steinemman S, Fiorellini JP, Fox CH, Stich H. Influence of surface characteristic on bone integration of titanium implants. A histomorphomertic study in miniature pigs. J Biomed Mater Res.1991;25:889-902.
26. Jagjit S, Rubens F, Monzur M, Jocelyne S. Osseointegration of standard and minidental implants: a histomorphometric comparison. Int J Implant Dent. 2017; 3:15.
27. Rebollal J, Soares GA, Vidigal GM Jr. Histomorphometric analysis of hydroxyapatite- coated implants in rabbits cortical bone using longitudinal and transverse histological sections. Implant Dent. 2010;19:137-43.
28. Yohei I, Masatsugu H, Tohru H, Chikahiro O. Surrounding tissue response to surface-treated zirconia implants. Materials. 2020;13:30.
29. Dawlat M, Moustafa A. Bioactive–hybrid–zirconia implant surface for enhancing osseointegration: an in vivo study. Int J Implant Dent. 2018;4:20.
30. Qiu C, Xiao X, Liu R. Biomimetic synthesis of spherical nano hydroxyapatite in the presence of polyethylene glycol. Ceram Int. 2008;34:1747-51.
31. Meejoo S, Maneeprakorn W, Winotai P. Phase and thermal stability of nanocrystalline hydroxyapatite prepared via microwave heating. Thermochim Acta. 2006;447:115–20.
32. Destainville A, Champion E, Bernache-Assollant D, Laborde E. Synthesis, characterization and thermal behavior of apatitic tricalcium phosphate. Mater Chem Phys. 2003;80:269–77.
33. Chalmers JM, Gaskin WF, Mackenzie MW. Crystallinity in poly (aryl-etherketone) plaques studied by multiple internal-reflection spectroscopy. Polymer Bulletin. 1984;11:433-5.
34. Prodanov L, Lamers E, Domanski M, Luttge R, Jansen JA, Walboomers XF. The effect of nanometric surface texture on bone contact to titanium implants in rabbit tibia. Biomaterials. 2013;34:2920–7.
35. Ahmet K, Serhat E, Volkan S, Burak Y, Mehmet A. Effect of various treatment modalities on surface characteristics and shear bond strengths of polyetherether ketone. J Prostho. 2017;29:136-41.
36. Minzhi Z, Haiyun L, Xiaochen L, Jie W, Jianguo J, Shu Y, et al. Response of human osteoblast to nHA/PEEK—quantitative proteomic study of bio-effects of nano-hydroxyapatite composite. Sci Rep. 2016;6:22832.
37. Pearce AI, Richards RG, Milz S, Schneider E, Pearce SG. Animal models for implant biomaterial research in bone: a review. Eur Cell Mater. 2007;13:1-10.
38. Mapara M, Thomas BS, Bhat KM. Rabbit as an animal model for experimental research. Dent Res J. 2012;9:111-8.
39. Masoud I, Shapiro F, Kent R, Moses A. A longitudinal study of the growth of the New Zealand white rabbit: cumulative and biweekly incremental growth rates for body length, body weight, femoral length, and tibial length. J Orthop Res. 1986;4:221-31.